Crossref Similarity Check
Powered by iThenticate

Reason- A Technical Journal
ISSN 2277-1654
Volume XXII 2023

COMPARATIVE ANALYSIS OF FOUR SVPWM SWITCHING TECHNIQUES FOR QZSI AND ITS EFFECT ON INDUCTOR CURRENT RIPPLE AND OUTPUT THD

Ayantika Guria[1], Sayantan Chowdhury[2] and Pritam Kumar Gayen[3]

Department of Electrical Engineering, Kalyani Government Engineering College, Kalyani- 741235
Email: [1]ayantika.guria99@gmail.com, [2]titinbabu@gmail.com and [3]pkgtar@gmail.com

Paper submitted on May 04 2024, Accepted after revision on November 05 2024
DOI : 10.21843/reas/2023/43-58/47348

Abstract: The different effects of variation of distribution of shoot-trough states in space vector pulse width modulation method of quasi Z-source inverter (qZSI) are the contribution of the proposed work. In this regard, the inductor current ripple and total harmonic distortion (THD) are considered as performance parameters. Shoot-through states are distributed throughout the total time period (T_{st}) to observe the current ripple of the inductor present in the impedance network of qZSI. Four different types of distributed shoot-through states have been developed in order to compare the amount of the inductor current ripple of the impedance network. The duration of shoot-through time period is split. These are positioned throughout T_{st} at equal and/or unequal intervals. The current ripple of the inductor varies with different shoot-through distributions for the same operating condition of the power circuit. Thus, the noticeable impact on the inductor current ripple is observed with the splitting proportions of shoot-through duration and their sequences. In addition to the inductor current ripple, the variations of THD values are investigated for the different SVPWM methods. The SVPWM methods are verified with various simulation studies.

Keywords: Quasi Z-Source Inverter, qZSI, Space Vector Pulse Width Modulation, SVPWM, Shoot through states, Inductor current ripple.

NOMENCLATURE

- P_{out} = Output Power
- V_{in}= Input Voltage
- V_{dc}= DC-Link Voltage
- V_0=Phase Voltage
- V_{ref}=Reference Voltage Vector
- V_{C_1}, V_{C_2} = Voltage Across respective Capacitors
- I_0= Output Current
- I_{dc} = DC-Link Current
- I_{L_1}, I_{L_2} = Current Across respective Inductors
- L_1, L_2=Inductors of Impedance Network of qZSI
- C_1, C_2= Capacitors of Impedance Network of qZSI
- L_f = Output Filter Inductor
- C_f = Output Filter Capacitor
- f_{sw} = Switching Frequency
- T_s= Switching Time Period
- M= Modulation Index
- D= Shoot-Through Duty Cycle
- B= Boosting Factor
- G = Overall Boosting Gain
- K_v= Ripple Factor of Capacitor Voltage
- K_i= Ripple Factor of Inductor Current
- T_1 = Time Interval for Active State
- T_2 = Time Interval for Active State
- T_0 = Time Interval for Zero State
- T_{st} =TotalTime Interval for Shoot Through State
- T_{st1} = Time Interval for Shoot Through State for method 4
- T_{st2} = Time Interval for Shoot Through State for method 4
- T_{st3} = Time Interval for Shoot Through State for method 4

- d_a = Duty Ratio of T_1
- d_b = Duty Ratio of T_2
- d_z = Duty Ratio of T_0
- ΔI_L=Peak-to-Peak Inductor Current Ripple
- K_v = Ripple Factor of Capacitor Voltage
- K_i = Ripple Factor of Inductor Current

1. INTRODUCTION

Nowadays, the demand for using emission-free and renewable-based sources of energy is increasing day-by-day, as the traditional resources of power generation are limited in nature and produce harmful end products. Power systems integrated with only renewable sources of power are difficult to operate as renewable sources of power like solar (PV), wind, fuel cells, and others are highly dependent on weather conditions [1]. Nowadays, green and clean energy are also in demand in transportation services. The demand for electric vehicles (EVs) is increasing worldwide. For operation of both renewable and EVs, two-stage converters are required, which consist of a DC-DC converter and a voltage or current source inverter (VSI/CSI). But the VSI and CSI can operate only in DC-AC buck mode or boost mode and have 6 active states and 2 zero states. For a flexible AC machine's operation over a wide speed range, an inverter with buck boost capability is required [2,3].

To achieve buck-boost capability in a single-stage inverter, Z-source inverters are used. As a single-stage system, Z-source inverters are more compact. It has an additional shoot-through state along with 8 operational states of traditional inverter. An impedance network present on the input side allows the inverter to operate both in short-circuit state and open circuit state [4]. The input current of the traditional Z-source inverter is discontinuous, whereas the input current drawn by qZSI is continuous [5]. The qZSI can be used with both sinusoidal pulse width modulation (SPWM) switching technique and space vector pulse width modulation (SVPWM) technique. One shoot-through interval can be applied in each SPWM switching cycle, whereas in SVPWM shoot-through time can be applied in several equal/unequal intervals of time, resulting in low current ripple of the inductor [6]. Shoot-through state in qZSI is achieved by shorting at least the upper and lower switches of one leg of the inverter, which steps up or steps down the output ac voltage [7]. As depicted in Fig. 1, the qZSI consists of an impedance network (combination of inductors, capacitors, and a diode) at the input and six Metal Oxide Semiconductor Field Effect Transistor (MOSFET)/Insulated Gate Bipolar Transistor (IGBT) switches [8].

The conventional SPWM method generates fundamental as well as harmonic voltages at the output of the inverter. Upon application of this harmonic voltage to the electric motors, it generates pulsating torque. With the advent of SVPWM, it is possible for the control of various motor-drives with reduced harmonics [9,10]. The modified SVPWM technique can improve the running speed of the system, and the common mode voltage can also be reduced by this [11]. In the case of PV cells, maximum output power from them can be obtained by implementing the SVPWM technique [12]. A modified SVPWM technique that addresses issues like synchronisation, independent control, and unintentional short circuiting in qZSI can give better efficiency than the conventional one

[13]. The qZSI is preferred for renewable and for EVs as it ailows a wide range of voltage input and provides buck boost capabiiity in a singie stage [14,15]. To controi the boosting factor with the heip of switching devices in qZSi by implementing shoot-through mode in a certain manner in turn reduces device stress but maximizes the boosting factor [16]. Two inductors are used in the impedance network of qZSi. The basic approach that is used to reduce the current ripple of the inductor and increase the compactness of qZSI is by increasing the switching frequency. But by increasing switching frequency, switching losses increase [17].

In this paper, the proposed work mainly investigates the comparison of minimization of inductor current ripple by implementing four different types of distributed shoot-through in equal and/or unequal intervals of time in total time period *Ts* of SVPWM switching cycles without changing the switching frequency. The effect on total harmonic distortion (THD) of the inverter output for four types of switching is also investigated in this work.

2. QUASI-Z SOURCE INVERTER (QZSI)

The block diagram of qZSI is depicted in Fig.1, the impedance network at the input consists of two inductors, two capacitor filters and a diode, the output of the impedance bridge is fed to the MOSFET/IGBT switches for DC to AC conversion. The output from the switches is fed to the load via LC filter in order to reduce harmonics at the output.

2.1.Operating states of qZSI

The two operating states of qZSI are shoot-through and active states as shown in Fig. 2. During shoot-through state, the DC-link bus is short circuited by turning on the inverter switchesof one or multiple legs of same phase. The voltage acrosspre-charged capacitor C_2 and C_2 releases its stored energy into the circuit, which in turn energizes the two inductors L_2 and L_2. The equations for the shoot through state (Fig. 2a) are given by Eq. (1) through Eq. (4).

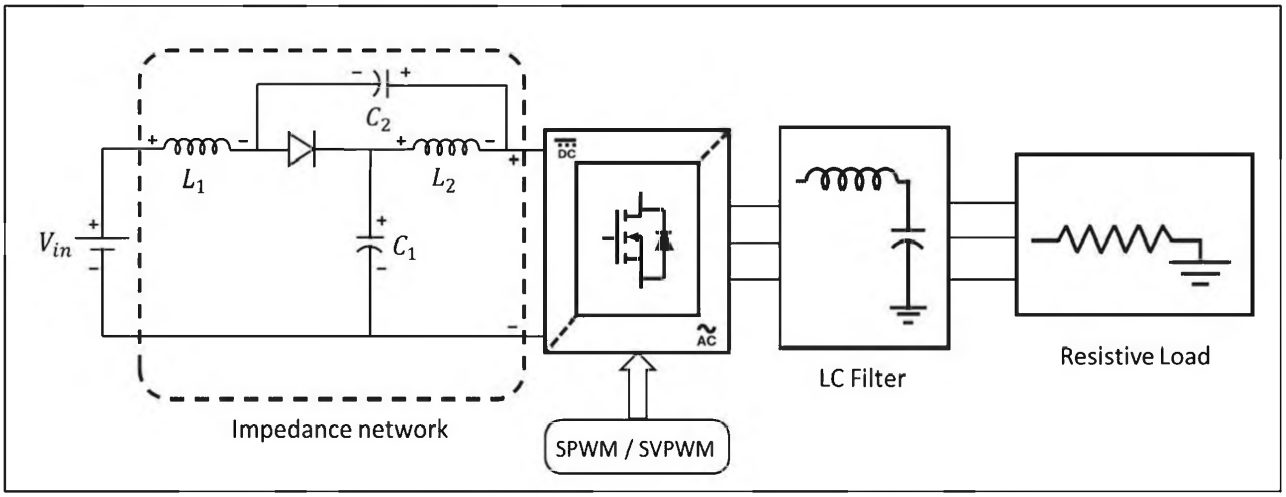


Fig. 1. Block diagram of Quasi Z-source inverter.

$$L_1 \frac{di_{L_1}(t)}{dt} = V_{in}(t) + V_{C_2}(t) \quad (1)$$

$$L_2 \frac{di_{L_2}(t)}{dt} = V_{C_2}(t) \quad (2)$$

$$C_1 \frac{dV_{C_1}(t)}{dt} = -I_{L_2}(t) \quad (3)$$

$$C_2 \frac{dV_{C_2}(t)}{dt} = -I_{L_1}(t) \quad (4)$$

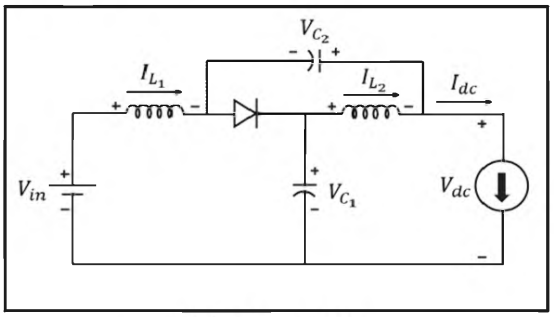
The qZSI delivers power to the load as well as the capacitors C_1 and C_1 gets charged during the active state. During active state, the energized inductors release the stored energy which gives dc link voltage boost at the input of inverter switch. The equations for the active state (Fig. 2b) are given by Eq. (5) through Eq. (8).

$$L_1 \frac{di_{L_1}(t)}{dt} = V_{in}(t) - V_{C_1}(t) \quad (5)$$

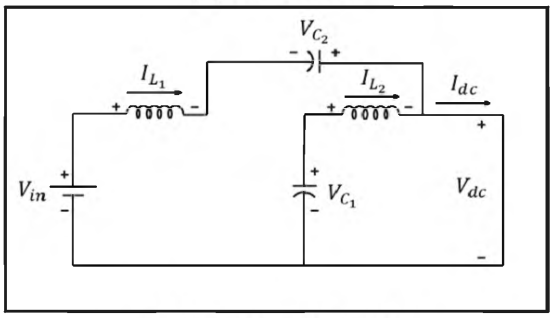
$$L_2 \frac{di_{L_2}(t)}{dt} = -V_{C_2}(t) \quad (6)$$

$$C_1 \frac{dv_{C_1}(t)}{dt} = -I_{dc}(t) + I_{L_1}(t) \quad (7)$$

$$C_2 \frac{dv_{C_2}(t)}{dt} = -I_{dc}(t) + I_{L_2}(t) \quad (8)$$



(a) Active state



(b) Shoot through state

Fig. 2. Equivalent circuit diagram of qZSI for active and shoot through states.

2.2. Design of qZSI

The topology of qZSI, shown in Fig. 1, can be designed according to Eq. (9) through Eq. (16) which are mentioned below

$$D = 1 - M \quad (9)$$

$$B = \frac{1}{1-2D} \quad (10)$$

$$V_{dc} = B * V_{in} \quad (11)$$

$$V_0 = M * B * \frac{V_{in}}{2} \quad (12)$$

$$V_0 = G * \frac{V_{in}}{2} \quad (13)$$

$$G = M * B \quad (14)$$

$$L = L_1 = L_2 = \frac{V_{in} * D * T_s}{2 * K_i * I_0} \quad (15)$$

$$C = C_1 = C_2 = \frac{I_0 * D * T_s}{2 * K_v * V_{in}} \quad (16)$$

The different voltage and current ratings of capacitors and inductors that are required to design the impedance network of qZSI can be calculated according to Eq. (17) through Eq. (19).

$$V_{C_1} = \frac{1-D}{1-2D} V_{in} \quad (17)$$

$$V_{C_2} = \frac{D}{1-2D} V_{in} \quad (18)$$

$$I_{L_1} = I_{L_2} = \frac{P}{V_{in}} \quad (19)$$

The DC link voltage can be calculated according to Eq. (22) which is basically the summation of the voltage appearing across the two capacitors C_2 and C_2.

$$V_{dc} = V_{C_1} + V_{C_2} \quad (20)$$

$$V_{dc} = \frac{1}{1-2D} V_{in} \quad (21)$$

$$V_{dc} = B * V_{in} \quad (22)$$

Theoretically, the duty ratio must be maintained from 0 to 0.5 for the qZSI.

3. SVPWM FOR QZSI

The SVPWM for qZSI is different from traditional VSI as shoot through states have to be included besides active states and zero states. The SVPWM offers the flexibility in implementing shoot through state as it can be distributed equally/unequally over one complete switching cycle. The methods discussed below incorporate equation for four types of SVPWM switching for qZSI are as follows:

3.1. Method 1

In this method, T_{st} has been divided into two equal parts and they are positioned within zero statesas shown in Fig.3. The time span of the active states is calculated according to Eq. (23) and Eq. (24), zero state is given by Eq. (25) and shoot through state is given by Eq. (26).

$$T_1 = \sqrt{3} * \frac{V_{ref}}{V_{dc}} * T_s * Sin\frac{(n+\pi)}{(3-\alpha)} \quad (23)$$

$$T_2 = \sqrt{3} * \frac{V_{ref}}{V_{dc}} * T_s * Sin\{\alpha - \frac{(n-1)*\pi}{3}\} \quad (24)$$

$$T_0 = T_s - T_1 - T_2 \quad (25)$$

$$T_{st} = D * T_s \quad (26)$$

The time interval of shoot through state (T_{st}) is equally divided into two parts and these are included in the timing calculation. The detailed calculation is shown in Table 1.

Table 1. Switching time calculation for qZSI for method 1.

Sector	Upper Switches (1,3,5)	Lower Switches(2,4,6)
1	S1=$T_1+T_2+T_0/2+T_{st}/2$ S3 = $T_2+T_0/2+T_{st}/2$ S5= $T_0/2+T_{st}/2$	S2=$T_1+T_2+T_0/2+T_{st}/2$ S4=$T_0/2+T_{st}/2$ S6= $T_1+T_0/2+T_{st}/2$
2	S1=$T_1+T_0/2+T_{st}/2$ S3 = $T_1+T_2+T_0/2+T_{st}/2$ S5= $T_0/2+T_{st}/2$	S2=$T_1+T_2+T_0/2+T_{st}/2$ S4 = $T_2+T_0/2+T_{st}/2$ S6= $T_0/2+T_{st}/2$
3	S1=$T_0/2+T_{st}/2$ S3 = $T_1+T_2+T_0/2+T_{st}/2$ S5= $T_2+T_0/2+T_{st}/2$	S2=$T_1+T_0/2+T_{st}/2$ S4 = $T_1+T_2+T_0/2+T_{st}/2$ S6= $T_0/2+T_{st}/2$
4	S1=$T_0/2+T_{st}/2$ S3 = $T_1+T_0/2+T_{st}/2$ S5= $T_1+T_2+T_0/2+T_{st}/2$	S2=$T_0/2+T_{st}/2$ S4 = $T_1+T_2+T_0/2+T_{st}/2$ S6= $T_2+T_0/2+T_{st}/2$
5	S1=$T_2+T_0/2+T_{st}/2$ S3 = $T_0/2+T_{st}/2$ S5= $T_1+T_2+T_0/2+T_{st}/2$	S2=$T_0/2+T_{st}/2$ S4= $T_1+T_0/2+T_{st}/2$ S6= $T_1+T_2+T_0/2+T_{st}/2$
6	S1=$T_1+T_2+T_0/2+T_{st}/2$ S3 =$T_0/2+T_{st}/2$ S5= $T_1+T_0/2+T_{st}/2$	S2=$T_2+T_0/2+T_{st}/2$ S4 = $T_0/2+T_{st}/2$ S6= $T_1+T_2+T_0/2+T_{st}/2$

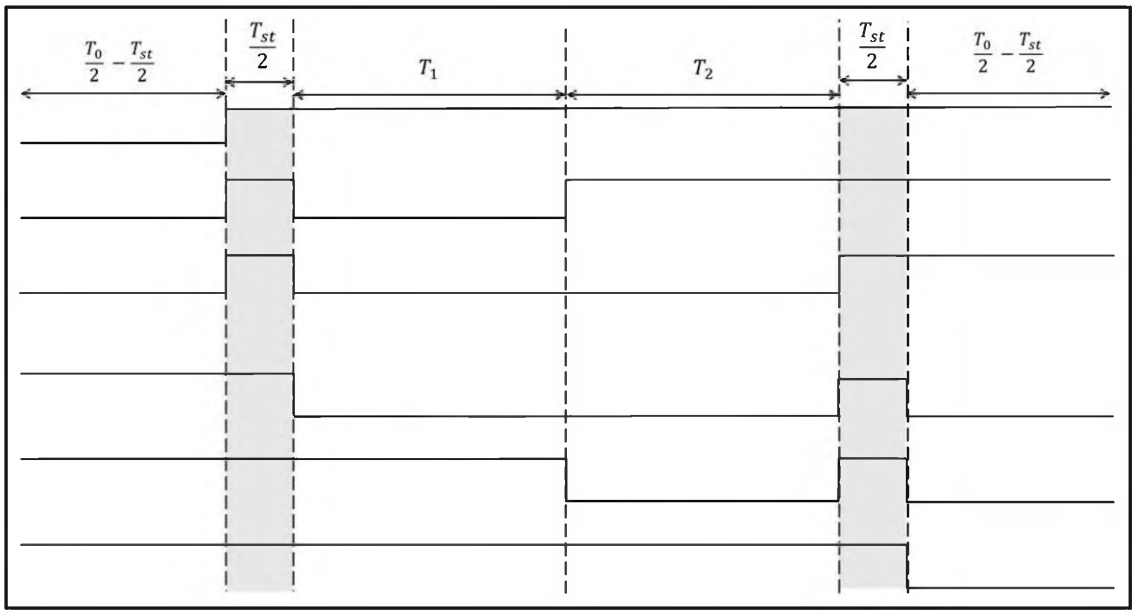


Fig. 3. Switching time diagram for method 1

of the active states is calculated according to Eq. (23) and Eq. (24), zero state is given by Eq. (25) and shoot through state is given by Eq. (26).

The time interval of shoot through state (T_{st}) is equally divided into two parts and these are included in the timing calculation. The detailed calculation is shown in Table 1.

$$T_1 = \sqrt{3}\left(\frac{V_{ref}}{V_{dc}}\right) * T_s * Sin(\frac{n\pi}{3-\alpha}) \quad (27)$$

$$T_2 = \sqrt{3}\left(\frac{V_{ref}}{V_{dc}}\right) * T_s * Sin\{\alpha - (n-1)\frac{\pi}{3}\} \quad (28)$$

$$T_0 = T_s - T_1 - T_2 \quad (29)$$

$$T_{st} = D * T_s \quad (30)$$

Table 2. Switching time calculation for qZSI for method 2.

Sector	Upper Switches (1,3,5)	Lower Switches(2,4,6)
1	S1=$T_1+T_2+T_0/2+T_{st}/2$ S3 = $T_2+T_0/2+T_{st}/2$ S5= $T_0/2+T_{st}/2$	S2=$T_1+T_2+T_0/2+T_{st}/2$ S4=$T_0/2+T_{st}/2$ S6= $T_1+T_0/2+T_{st}/2$
2	S1=$T_1+T_0/2+T_{st}/2$ S3 = $T_1+T_2+T_0/2+T_{st}/2$ S5= $T_0/2+T_{st}/2$	S2=$T_1+T_2+T_0/2+T_{st}/2$ S4 = $T_2+T_0/2+T_{st}/2$ S6= $T_0/2+T_{st}/2$
3	S1=$T_0/2+T_{st}/2$ S3 = $T_1+T_2+T_0/2+T_{st}/2$ S5= $T_2+T_0/2+T_{st}/2$	S2=$T_1+T_0/2+T_{st}/2$ S4 = $T_1+T_2+T_0/2+T_{st}/2$ S6= $T_0/2+T_{st}/2$
4	S1=$T_0/2+T_{st}/2$ S3 = $T_1+T_0/2+T_{st}/2$ S5= $T_1+T_2+T_0/2+T_{st}/2$	S2=$T_0/2+T_{st}/2$ S4 = $T_1+T_2+T_0/2+T_{st}/2$ S6= $T_2+T_0/2+T_{st}/2$
5	S1=$T_2+T_0/2+T_{st}/2$ S3 = $T_0/2+T_{st}/2$ S5= $T_1+T_2+T_0/2+T_{st}/2$	S2=$T_0/2+T_{st}/2$ S4= $T_1+T_0/2+T_{st}/2$ S6= $T_1+T_2+T_0/2+T_{st}/2$
6	S1=$T_1+T_2+T_0/2+T_{st}/2$ S3 =$T_0/2+T_{st}/2$ S5= $T_1+T_0/2+T_{st}/2$	S2=$T_2+T_0/2+T_{st}/2$ S4 = $T_0/2+T_{st}/2$ S6= $T_1+T_2+T_0/2+T_{st}/2$

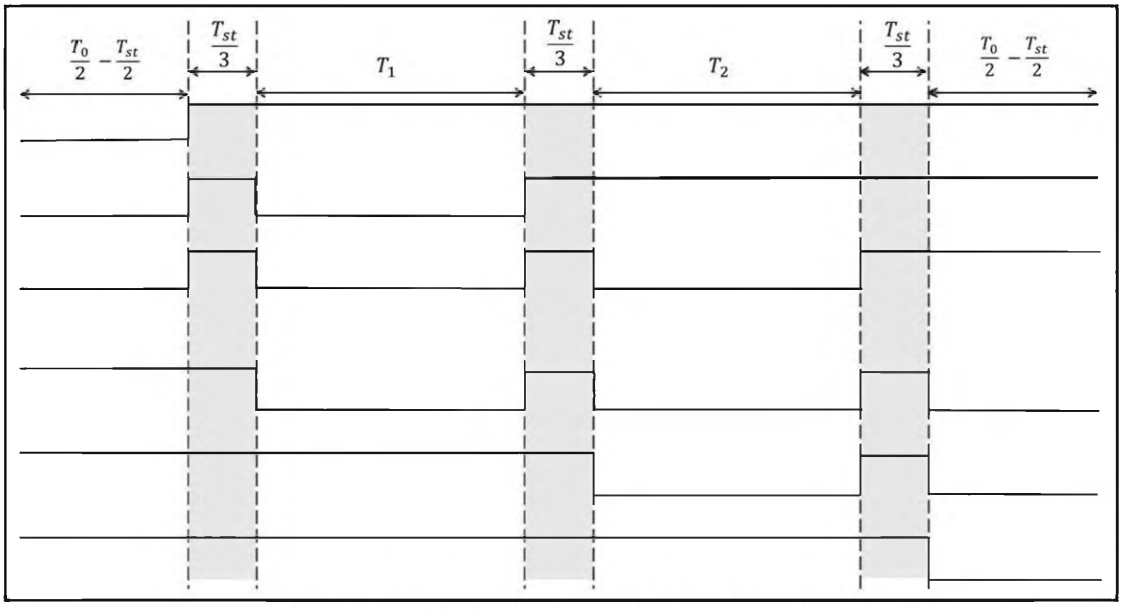


Fig. 4. Switching time diagram for method 2

3.3. Method 3

In this method, T_{st} has been divided into four equal parts and they are positioned in zero states and in between the active states as shown in Fig. 5. The time span of the active states is calculated according to Eq. (31) and Eq. (32), zero state is given by Eq. (33) and shoot through state is given by Eq. (34).

$$T_1 = \sqrt{3}\left(\frac{V_{ref}}{V_{dc}}\right) * T_s * Sin(\frac{n\pi}{3-\alpha}) \quad (31)$$

$$T_2 = \sqrt{3}\left(\frac{V_{ref}}{V_{dc}}\right) * T_s * Sin\{\alpha - (n-1)\frac{\pi}{3}\} \quad (32)$$

$$T_0 = T_s - T_1 - T_2 \quad (33)$$

$$T_{st} = D * T_s \quad (34)$$

The time interval of shoot through state (T_{st}) is equally divided into four parts and these are included in the timing calculation. The detailed calculation is presented in Table 3.

The time interval of shoot through state (T_{st})

Table 3. Switching time calculation for qZSI for method 3.

Sector	Upper Switches (1,3,5)	Lower Switches(2,4,6)
1	S1=T_1+T_2+T_0/2+T_{st}/2 S3 = T_2+T_0/2+T_{st}/2 S5= T_0/2+T_{st}/2	S2=T_1+T_2+T_0/2+T_{st}/2 S4=T_0/2+T_{st}/2 S6= T_1+T_0/2+T_{st}/2
2	S1=T_1+T_0/2+T_{st}/2 S3 = T_1+T_2+T_0/2+T_{st}/2 S5= T_0/2+T_{st}/2	S2=T_1+T_2+T_0/2+T_{st}/2 S4 = T_2+T_0/2+T_{st}/2 S6= T_0/2+T_{st}/2
3	S1=T_0/2+T_{st}/2 S3 = T_1+T_2+T_0/2+T_{st}/2 S5= T_2+T_0/2+T_{st}/2	S2=T_1+T_0/2+T_{st}/2 S4 = T_1+T_2+T_0/2+T_{st}/2 S6= T_0/2+T_{st}/2
4	S1=T_0/2+T_{st}/2 S3 = T_1+T_0/2+T_{st}/2 S5= T_1+T_2+T_0/2+T_{st}/2	S2=T_0/2+T_{st}/2 S4 = T_1+T_2+T_0/2+T_{st}/2 S6= T_2+T_0/2+T_{st}/2
5	S1=T_2+T_0/2+T_{st}/2 S3 = T_0/2+T_{st}/2 S5= T_1+T_2+T_0/2+T_{st}/2	S2=T_0/2+T_{st}/2 S4= T_1+T_0/2+T_{st}/2 S6= T_1+T_2+T_0/2+T_{st}/2
6	S1=T_1+T_2+T_0/2+T_{st}/2 S3 =T_0/2+T_{st}/2 S5= T_1+T_0/2+T_{st}/2	S2=T_2+T_0/2+T_{st}/2 S4 = T_0/2+T_{st}/2 S6= T_1+T_2+T_0/2+T_{st}/2

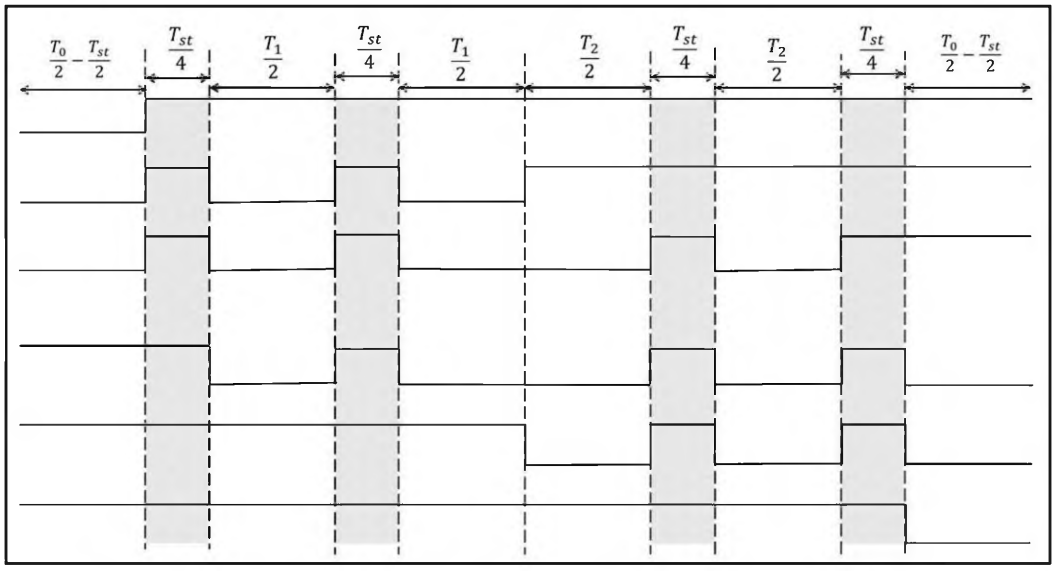


Fig. 5. Switching time diagram for method 3

3.4. Method 4

In this method, the time interval of shoot through state (T_{st}) has been divided into threeunequal parts (T_{st1}, T_{st2}, and T_{st3},) and they are positioned in zero states and in between the active states as shown in Fig 6. The time span of the active states is calculated according to Eq. (38) and Eq. (39), zero state is given by Eq. (40) and shoot through state is given by Eq. (41) through Eq. (44).

The time interval of shoot through state (T_{st}) is divided unequally into three parts and these are included in the timing calculation. The detailed calculation is given in Table 4.

$$d_a = \sqrt{3}\left(\frac{V_{ref}}{V_{dc}}\right) * Sin\left(\frac{n\pi}{3-a}\right) \quad (35)$$

$$d_b = \sqrt{3}\left(\frac{V_{ref}}{V_{dc}}\right) * Sin\{\alpha - (n-1)\frac{\pi}{3}\} \quad (36)$$

$$d_z = 1 - d_a - d_b \quad (37)$$

$$T_1 = d_a * T_s \quad (38)$$

$$T_2 = d_b * T_s \quad (39)$$

$$T_0 = d_z * T_s \quad (40)$$

$$T_{st} = D * T_s \quad (41)$$

$$T_{st1} = \frac{(d_a+d_z)*D*T_s}{2} \quad (42)$$

$$T_{st3} = \frac{(d_b+d_z)*D*T_s}{2} \quad (43)$$

$$T_{st2} = T_{st} - T_{st1} - T_{st3} \quad (44)$$

Table 4. Switching time calculation for qZSI for method 4.

Sector	Upper Switches (1,3,5)	Lower Switches (2,4,6)
1	$S1 = T_1 + T_2 + T_0/2 + T_{st1} + T_{st2}/2$ $S3 = T_2 + T_0/2 + T_{st1} + T_{st2}/2$ $S5 = T_0/2 + T_{st1} + T_{st2}/2$	$S2 = T_1 + T_2 + T_0/2 + T_{st3} + T_{st2}/2$ $S4 = T_0/2 + T_{st3} + T_{st2}/2$ $S6 = T_1 + T_0/2 + T_{st3} + T_{st2}/2$
2	$S1 = T_1 + T_0/2 + T_{st1} + T_{st2}/2$ $S3 = T_1 + T_2 + T_0/2 + T_{st1} + T_{st2}/2$ $S5 = T_0/2 + T_{st1} + T_{st2}/2$	$S2 = T_1 + T_2 + T_0/2 + T_{st3} + T_{st2}/2$ $S4 = T_2 + T_0/2 + T_{st3} + T_{st2}/2$ $S6 = T_0/2 + T_{st3} + T_{st2}/2$
3	$S1 = T_0/2 + T_{st1} + T_{st2}/2$ $S3 = T_1 + T_2 + T_0/2 + T_{st1} + T_{st2}/2$ $S5 = T_2 + T_0/2 + T_{st1} + T_{st2}/2$	$S2 = T_1 + T_0/2 + T_{st3} + T_{st2}/2$ $S4 = T_1 + T_2 + T_0/2 + T_{st3} + T_{st2}/2$ $S6 = T_0/2 + T_{st3} + T_{st2}/2$
4	$S1 = T_0/2 + T_{st1} + T_{st2}/2$ $S3 = T_1 + T_0/2 + T_{st1} + T_{st2}/2$ $S5 = T_1 + T_2 + T_0/2 + T_{st1} + T_{st2}/2$	$S2 = T_0/2 + T_{st3} + T_{st2}/2$ $S4 = T_1 + T_2 + T_0/2 + T_{st3} + T_{st2}/2$ $S6 = T_2 + T_0/2 + T_{st3} + T_{st2}/2$
5	$S1 = T_2 + T_0/2 + T_{st1} + T_{st2}/2$ $S3 = T_0/2 + T_{st1} + T_{st2}/2$ $S5 = T_1 + T_2 + T_0/2 + T_{st1} + T_{st2}/2$	$S2 = T_0/2 + T_{st3} + T_{st2}/2$ $S4 = T_1 + T_0/2 + T_{st3} + T_{st2}/2$ $S6 = T_1 + T_2 + T_0/2 + T_{st3} + T_{st2}/2$
6	$S1 = T_1 + T_2 + T_0/2 + T_{st1} + T_{st2}/2$ $S3 = T_0/2 + T_{st1} + T_{st2}/2$ $S5 = T_1 + T_0/2 + T_{st1} + T_{st2}/2$	$S2 = T_2 + T_0/2 + T_{st3} + T_{st2}/2$ $S4 = T_0/2 + T_{st3} + T_{st2}/2$ $S6 = T_1 + T_2 + T_0/2 + T_{st3} + T_{st2}/2$

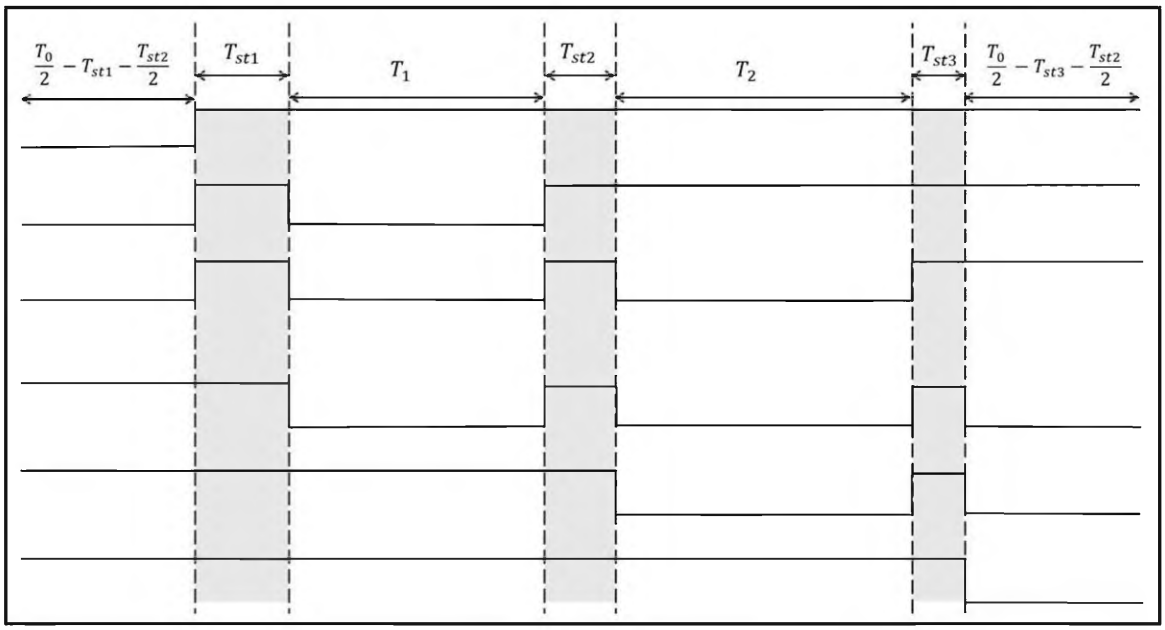


Fig. 6. Switching time diagram for method 4

4. SYSTEM SPECIFICATIONS

The specifications of the system on which the simulations have been performed to acquire the results is mentioned in Table 5.

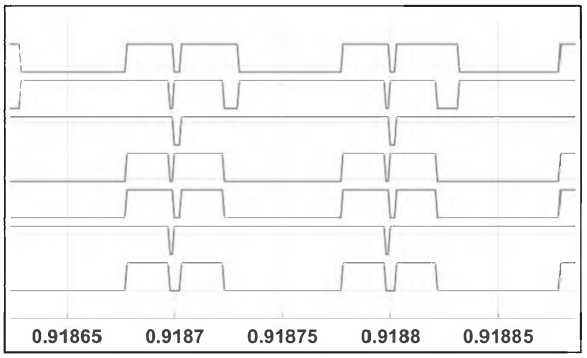
Table 5. Specifications of the System.

Parameters	Value
P_{out}	20 kW
f_{sw}	10 kHz
V_{in}	220 V
M	0.602
D	0.398
B	4.9
L_f	3 mH
C_f	5 μF
$L_1 = L_2$	2.1309 mH
$C_1 = C_2$	74.3 μF
K_V	0.05
K_i	0.05

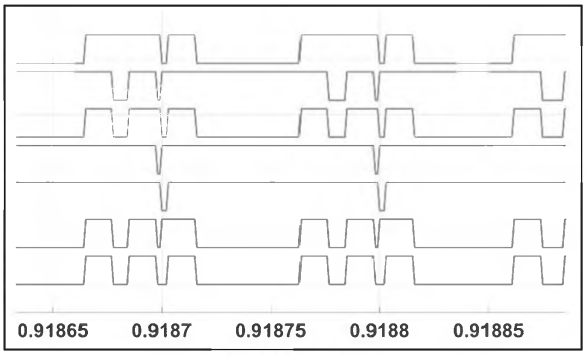
5. RESULTS

The proposed work has been carried out in MATLAB R2021a. The various results obtained are shown and discussed below.

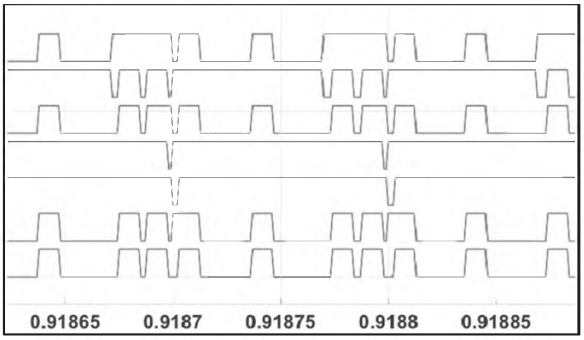
The four SVPWM switching techniques for qZSI as mentioned above, is depicted in Fig. 7 which is obtained from scope during simulation.



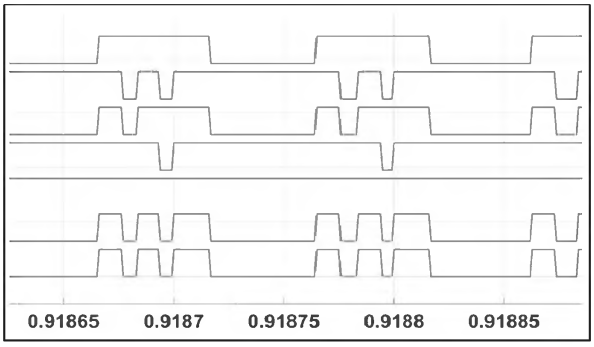
(a) Method 1



(b) Method 2



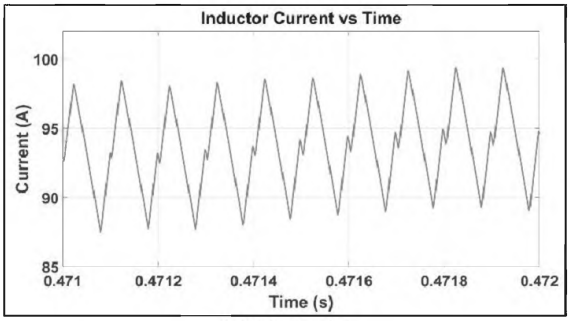
(c) Method 3



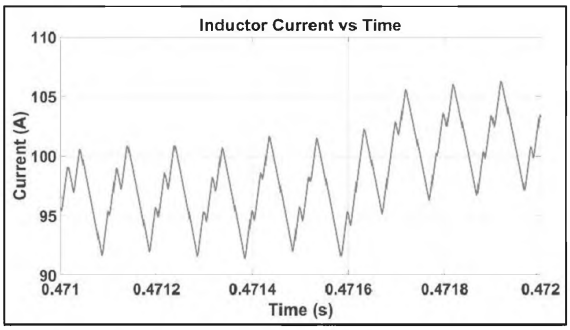
(d) Method 4

Fig. 7. Switching signals for four methods

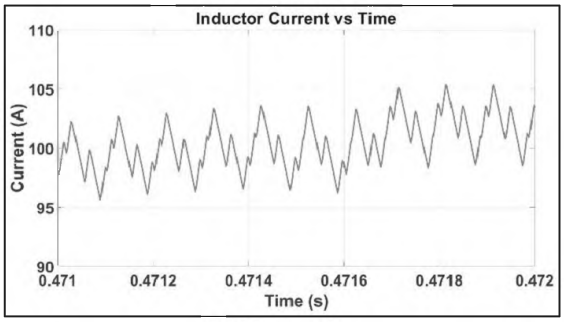
The inductor current ripples on application of the above mentioned four methods to qZSI are shown in Fig. 8.



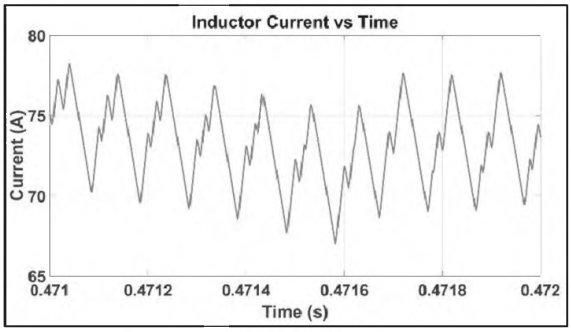
(a) Method 1



(b) Method 2



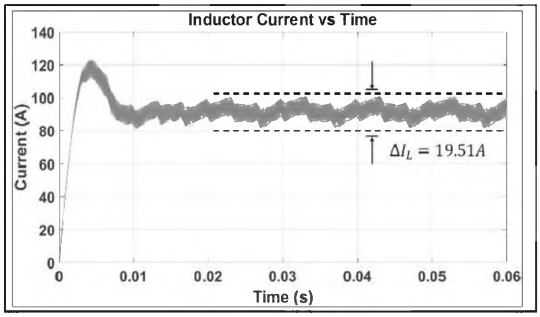
(c) Method 3



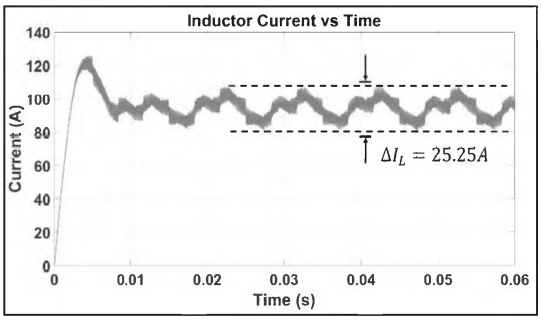
(d) Method 4

Fig. 8. Inductor current response for four switching techniques

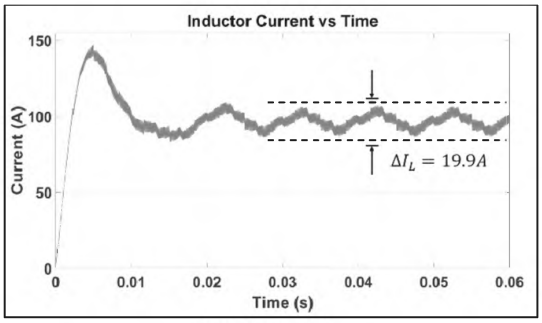
Effect on inductor current ripple on applica-tion of above mentioned four switching techniques for qZSI is depicted in Fig.9.



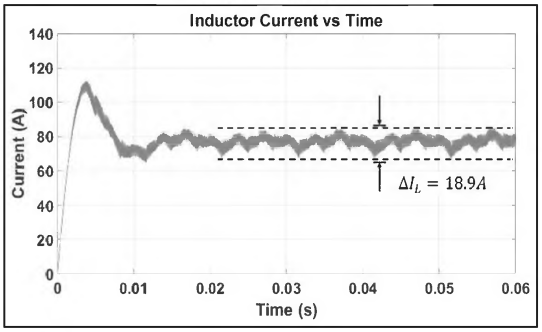
(a) Method 1



(b) Method 2



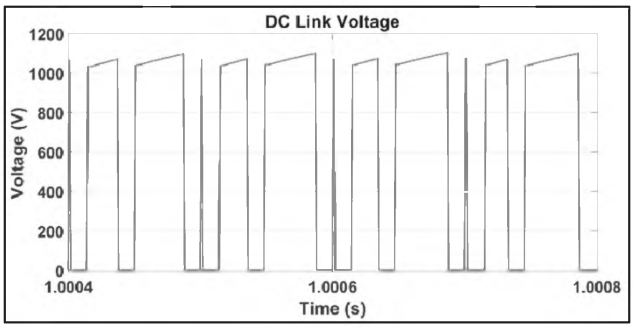
(c) Method 3



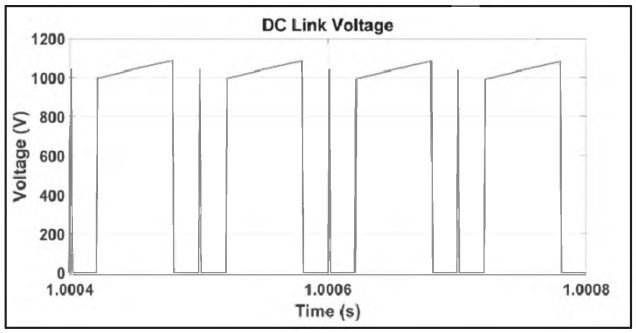
(d) Method 4

Fig. 9. Inductor current ripple response for four methods

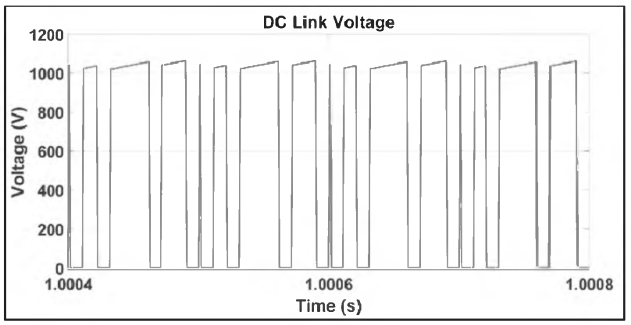
The DC link voltage response on application of the above mentioned four methods on qZSI is shown in Fig.10.



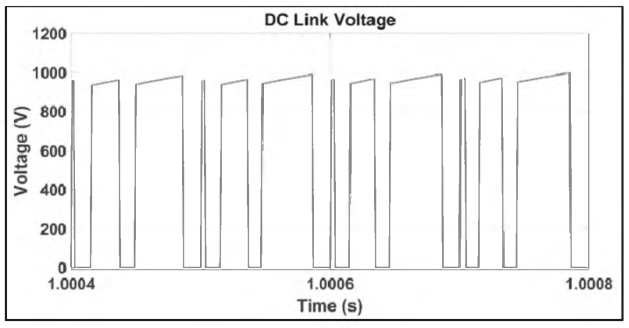
(b) Method 2



(a) Method 1



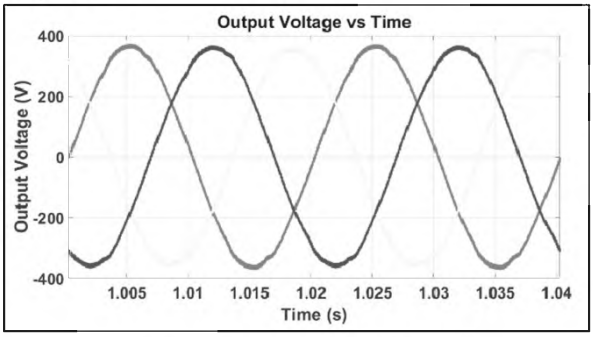
(c) Method 3

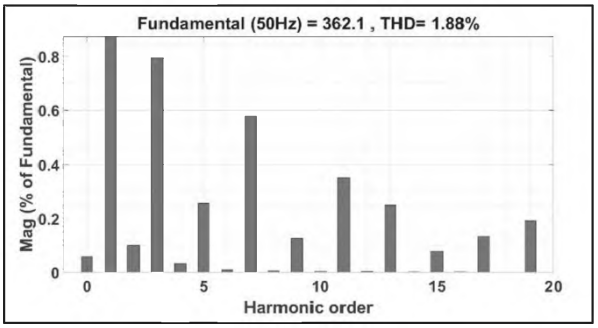


(d) Method 4

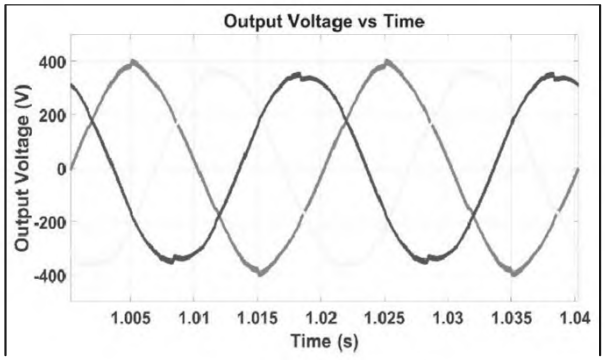
Fig. 10. DC link Voltage response for four methods.

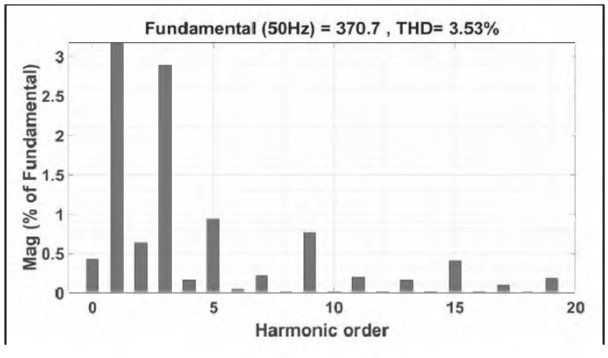
The output voltage waveform and its respective THDs for four switching techniques applied on qZSI is shown in Fig. 11.



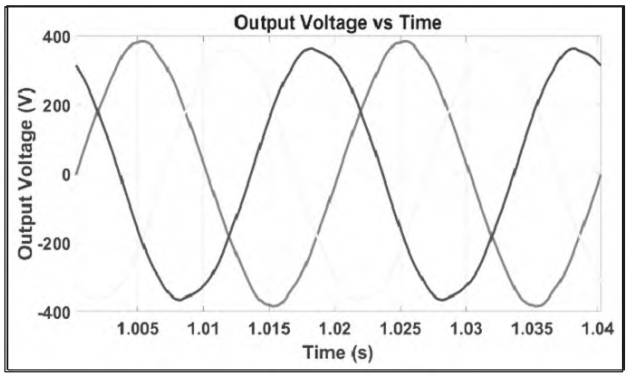


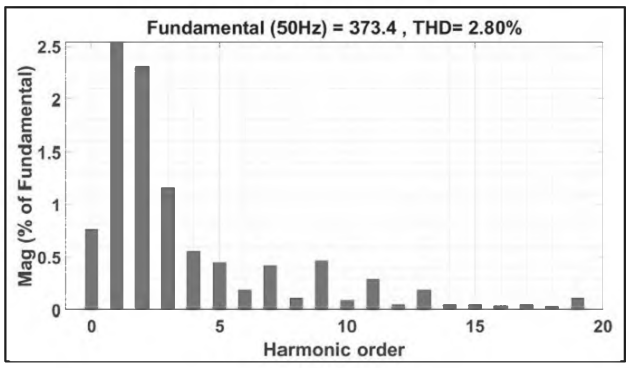
(a) Method 1



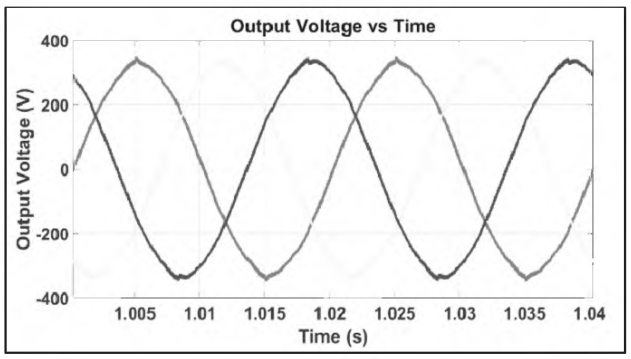


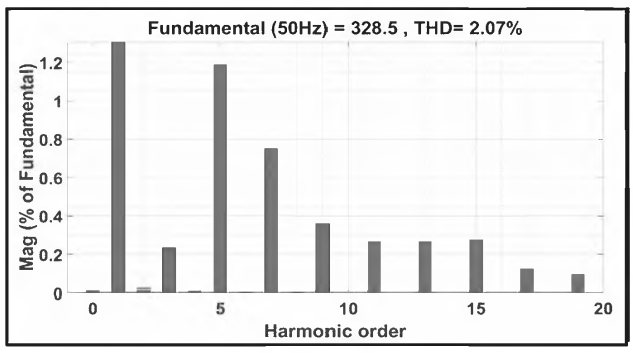
(b) Method 2





(c) Method 3





(d) Method 4

Fig. 11. Output voltage and their corresponding THD for four methods

6. CONCLUSION

The above work is conducted in order to study the effects of different SVPWM switching methods of qZSI. The work carried out in this paper mainly focuses on the effect of distributed shoot through placed at equal/unequal intervals of SVPWM switching cycles on current ripple of the inductors in the impedance network of qZSI. The shoot through durations have been implemented at various intervals keeping the boosting factor and the power circuit unchanged. From the above results, it is found that the increase in the number of shoot through distribution between active states and zero states has a noticeable impact on the inductor current ripple and the THD of the output voltage of the qZSI. As depicted in Fig. 11, it is found that the THD is within the permissible range i.e. 1% - 5% for the above-mentioned methods.The inductor current ripple for method 4 is 18.9 Ampere which is least among the four methods and the THD is 2.07% which lies within permissible range. But the inductor current ripple for method 2 is maximum as well as its THD is 3.53% which is highest among the four methods. The experimental validations and further investigations on the losses and efficiency of qZSI with the different SVPWM methods may be done in future research works.

REFERENCE

[1] Liu, Y., Ge, B., Ferreira, F. J. T. E., de Almeida, A. T. and Abu-Rub, H., Modeling and SVPWM Control of Quasi-Z-Source Inverter, 11th International Conference on Electrical Power Quality and Utilisation, Lisbon, Portugal, 2011, pp. 1-7, DOI: 10.1109/EPQU.2011.6128914.

[2] Liu, J., Hu, J. and Xu, L., A Modified Space Vector PWM for Z-source Inverter-Modeling and Design, 2005 International Conference on Electrical Machines and Systems, Nanjing, China, 2005, pp. 1242-1247, Vol. 2, DOI: 10.1109/ICEMS. 2005. 202746.

[3] Anderson, J. and Peng, F. Z., A Class of Quasi-Z-Source Inverters, 2008 IEEE Industry Applications Society Annual Meeting, Edmonton, AB, Canada, 2008, pp. 1-7, DOI: 10.1109/08IAS.2008.301.

[4] Liu, W., Yang, Y., Kerekes, T. And Blaabjerg, F., Generalized Space Vector Modulation for Ripple Current Reduction in Quasi-Z-Source Inverters, IEEE Transactions on Power Electronics, Vol. 36, No. 2, pp. 1730-1741, Feb. 2021, DOI: 10.1109/TPEL. 2020.3009866.

[5] Liu, W., Yang, Y., Kerekes, T., Vinnikov, D. and Blaabjerg, F., Inductor Current Ripple Analysis and Reduction for Quasi-Z-Source Inverters with an Improved ZSVM6 Strategy, IEEE Transactions on Power Electronics, Vol. 36, No. 7, pp. 7693-7704, July 2021, DOI: 10.1109/TPEL.2020. 3043102.

[6] Liu, W., Yang, Y., Kerekes, T. and Blaabjerg, F., Current Ripple Reduction for the Quasi-Z-Source Inverter with Modified Space-Vector PWM Strategy, 2020 IEEE Energy Conversion Congress and Exposition (ECCE), Detroit, MI, USA, 2020, pp. 1867-1872, DOI: 10.1109/ECCE44975. 2020.9236156.

[7] Jyothi, J. C., Salini, M. V. and Sreedevi, K. P., A Novel Space Vector PWM of Z-Source Inverter With Minimum Inductor Current Ripple, Asian Journal of Engineering and Technology, Vol. 3, No. 4, Aug. 2015.

[8] Peng, F. Z., Z-source inverter, IEEE Transactions on Industry Applications, Vol. 39, No. 2, pp. 504-510, March-April 2003, DOI: 10.1109/TIA.2003.808920.

[9] Kumar, T. V. and Rao, S. S., Switching State Algorithm for Space Vector Pulse Width Modulation (SVPWM), 7th Mediterranean Conference and Exhibition on Power Generation, Transmission, Distribution and Energy Conversion (MedPower 2010), Agia Napa, 2010, pp. 1-6, DOI: 10.1049/cp.2010.0913.

[10] Patidar, K. and Umarikar, A. C., A Space Vector PWM Signal Generation for Z-Source Inverter Using only Sampled Amplitudes of reference Phase Voltages with a Unified Method to Implement Different Shoot through Strategies, 2012 IEEE International Conference on Power Electronics, Drives and Energy Systems (PEDES), Bengaluru, India, 2012, pp. 1-5, DOI: 10.1109/PEDES.2012.6484427.

[11] G. Zhang and Y. Liu, A Modified SVPWM Algorithm for Quasi-Z-Source Inverter, 2022 6th International Conference on Power and Energy Engineering (ICPEE), Shanghai, China, 2022, pp. 191-196, DOI: 10.1109/ICPEE56418.2022.10050296.

[12] Shines, T. S. and Ramamoorthy, S., Quasi Z-source Inverter using Space Vector Modulation and Sine PWM Method, International Journal of Recent Technology and Engineering , Vol. 8, No. 2, July 2019.

[13] Grgic, I., Basic, M., Vukadinovic, D. and Marinovic, I., Novel Space-Vector PWM Schemes for Enhancing Efficiency and Decoupled Control in Quasi-Z-Source Inverters, Department of Power Engineering, Faculty of Electrical Engineering, Mechanical Engineering and Naval Architecture, University of Split, 21000 Split, Croatia, Published: 13 March 2024.

[14] Li, Y., Anderson, J., Peng, F. Z. and Liu, D., Quasi-Z-Source Inverter for Photovoltaic

Power Generation Systems, 2009 Twenty-Fourth Annual IEEE Applied Power Electronics Conference and Exposition, Washington, DC, USA, 2009, pp. 918-924, DOI: 10.1109/APEC.2009.4802772.

[15] Liske, A., Clos, G. and Braun, M., Analysis and modeling of the Quasi-Z-Source-Inverter, IECON 2011-37th Annual Conference of the IEEE Industrial Electronics Society, Melbourne, VIC, Australia, 2011, pp. 1197-1202, DOI: 10.1109/IECON.2011.6119479.

[16] Chowdhury, V. R. and Saritha, B., Analysis and Design of Impedance Network of Quasi Z-source Inverter, IEEE Sponsored 2nd International Conference on Power, Control and Embedded Systems (ICPCES– 2014), February 27–28, 2014, Anna University Guindy, Chennai, India.

[17] Iijima, R., Isobe, T. and Tadano, H., Optimized Short-Through Time Distribution for Inductor Current Ripple Reduction in Z-Source Inverters Using Space-Vector Modulation, IEEE Transactions on Industry Applications, Vol. 55, No. 3, pp. 2922-2930, May-June 2019, DOI: 10.1109/TIA.2019.2898848.